



Synthesis, SAR and biological evaluation of 1,6-disubstituted-1*H*-pyrazolo [3,4-*d*]pyrimidines as dual inhibitors of Aurora kinases and CDK1

Jean-Yves Le Brazidec^{a,*}, Angela Pasis^a, Betty Tam^a, Christina Boykin^a, Cheryl Black^a, Deping Wang^b, Gisela Claassen^a, Jer-Hong Chong^a, Jianhua Chao^a, Junhua Fan^a, Khanh Nguyen^a, Laura Silvian^{a,b}, Leona Ling^b, Lin Zhang^a, Michael Choi^{a,b}, Min Teng^a, Nuzhat Pathan^a, Shuo Zhao^a, Tony Li^a, Art Taveras^b

^a Biogen Idec, 5200 Research Place, San Diego, CA 92122, USA

^b Biogen Idec, 12 Cambridge Center, Cambridge, MA 02142, USA

ARTICLE INFO

Article history:

Received 26 October 2011

Revised 5 January 2012

Accepted 9 January 2012

Available online 18 January 2012

Keywords:

Aurora kinase
Cyclin dependent kinase
Cell cycle arrest
Pyrazolopyrimidine
Cytotoxicity

ABSTRACT

Since the early 2000s, the Aurora kinases have become major targets of oncology drug discovery particularly Aurora-A and Aurora-B kinases (AKA/AKB) for which the selective inhibition in cells lead to different phenotypes. In addition to targeting these Aurora kinases involved in mitosis, CDK1 has been added as a primary inhibition target in hopes of enhancing the cytotoxicity of our chemotypes harboring the pyrazolopyrimidine core. SAR optimization of this series using the AKA, AKB and CDK1 biochemical assays led to the discovery of the compound **7h** which combines strong potency against the 3 kinases with an acceptable microsomal stability. Finally, switching from a primary amide to a two-substituted pyrrolidine amide gave rise to compound **15a** which exhibited the desired AKA/CDK1 inhibition phenotype in cells but showed moderate activity in animal models using HCT116 tumor cell lines.

© 2012 Elsevier Ltd. All rights reserved.

The modulation of cell cycle by targeting kinases responsible for regulating cancer cells has been the object of intense research which resulted in the identification of putative targets such as cyclin dependant kinase 1 (CDK1)¹ and Aurora-A (AKA) and Aurora-B (AKB) kinases.² These kinases are often over-expressed³ in numerous cancer types and their specific inhibition by gene silencing or small molecule treatment leads to mitotic arrest and eventual cell death. In cells, CDK1 is functional when associated with a regulatory subunit such as cyclin A or cyclin B depending on the progress of the cell cycle toward mitosis.¹ During mitosis, AKA complexed with TPX2⁴ regulates centrosome separation and mitotic spindle formation while AKB complexed with INCENP⁵ is important in chromatid alignment and cytokinesis.

In an effort to enhance the cytotoxic effect associated with selective inhibition of only one of these three kinases, we focused our program on the development of a dual inhibitor of CDK1 and AKA. In addition to the work previously published on the pan-CDK/AKA inhibitor, JNJ7706621,⁶ this hypothesis was supported by results of an in vitro experiment combining a selective AKA inhibitor, MLN8054, with a selective CDK1 inhibitor, RO3306, in a 5-day MTS assay measuring the viability of HCT116 cells. The

combination treatment showed higher cytotoxicity and less neutropenia, as measured by the CFU-GM ratio (a measure of neutropenic effect), compared to each of the inhibitors alone (Table 1).

We embarked on optimizing the 1,6-disubstituted-1*H*-pyrazolo[3,4-*d*]pyrimidine chemotype to enable it to bind both CDK1 and Aurora kinases. This was derived from a homologous chemotype, 2,8-disubstituted-pyrido[2,3-*d*]pyrimidin-7(8*H*)-one, optimized for inhibition of CDK2 and CDK4 by Vanderwel et al.⁷

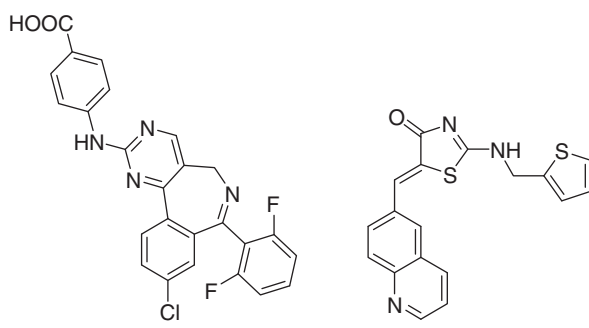
As previously reported,⁸ the synthesis of the pyrazolo-pyrimidine series started with the coupling between the thiomethyl pyrazolopyrimidine **1** and alicyclic alcohols (ROH) leading to the intermediates **2 (a–i)** (Scheme 1). After oxidation of these latter with *m*-CPBA, the sulfones **3 (a–i)** were condensed with the methyl 3-amino-pyrrole-carboxylate **4** under basic conditions to give the methyl esters **5 (a–i)** which were hydrolyzed into the key carboxylic acids **6 (a–i)** in good overall yield. Treated with either ammonium carbonate in the presence of (BOC)₂O or with a secondary amine under standard amide coupling conditions, the acids **6 (a–i)** were converted, respectively, into the primary amides **7 (a–i)** and the pyrrolidine amides **8 to 16** in acceptable yields.

In addition to increasing the biochemical potency against AKA and CDK1, a second goal of this study was to design a compound with better pharmaceutical properties by limiting its lipophilicity (CLogP), which is an important molecular property that has been

* Corresponding author.

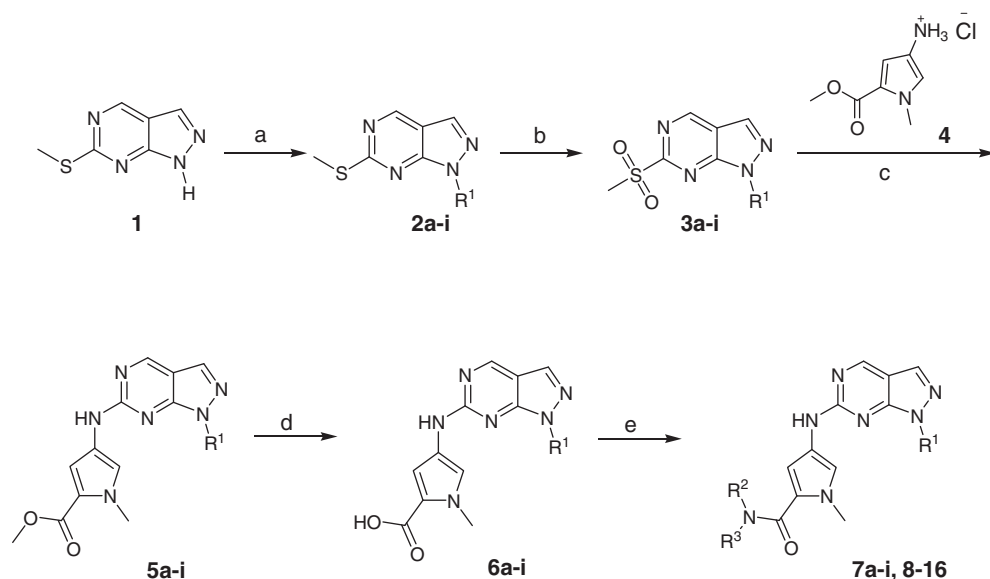
E-mail address: jean@chempartner.com (J.-Y. Le Brazidec).

Table 1
Combination of MLN8054 and RO3306 in MTS and neutropenia assays



Compd	AKA ^a IC ₅₀ (μM)	CDK1 ^a IC ₅₀ (μM)	HCT116 ^a IC ₅₀ (μM)	CFU-GM ratio ¹³
RO3306	>10	0.019	3.2	16.7
MLN8054	0.0015	>100	0.69	4.5
RO3306 + MLN8054	–	–	0.14	1.9

^a For assay descriptions, see Ref. 9.



Scheme 1. Reagents and conditions: (a) ROH, DIAD, PPh₃, THF, –70 °C to rt, 30–80%; (b) *m*-CPBA, DCM, rt, 95%; (c) **4**, K₂CO₃, DMSO, 80 °C; (d) KOH 5 N, MeOH/dioxane, 90%; (e) NH₄HCO₃, (BOC)₂O, pyridine, rt, 30–70% or R²R³NH, HATU, DIEA, THF, 50 °C, 50–80%.

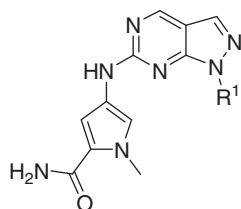
correlated with drug-likeness.⁹ During the optimization of this pyrazolo[3,4-*d*]pyrimidine series, the nature of R¹ was first modified in order to maximize its interactions with the lipophilic side chains from the amino acid residues such as Leu210, Leu263 and Phe275 lining the ribose binding pocket.¹⁰ In Table 2, the results showed that the isopropyl group conferred weak activity against AKA, AKB and CDK1 in compound **7a** but also conferred an improvement in metabolic stability. Increasing the size and the lipophilicity of R¹ by replacement of the isopropyl with a monocyclic ring (**7g** and **7e**), spirobicyclic rings (**7b** and **7f**), fused bicyclic rings (**7d**, **7h** and **7i**) and tricyclic rings (**7c**) led to a dramatic potency enhancement but accompanied with a significant loss in metabolic stability. The exception was compound **7h**; it maintained a % Qh under 70% and reasonable potency.

We then focused our attention on the amide moiety connected to the *N*-methyl 3-amino-pyrrole group to further improve potency while retaining reasonable metabolic stability. The *N*-methyl 3-amino-pyrrole is a key pharmacophore replacing the 4-sulfon-

amide-anilinyll group from the previous series.⁹ In order to improve the overall kinase selectivity profile, the two-substituted pyrrolidine amides were investigated (Table 3). Dimethylaminocarbonyl or methylaminomethyl substituents (**8**, **9**) led to weak activity against CDK1 and AKA which translated into reduced activity in cells. For the other substituents, the IC₅₀s in the biochemical assay against AKA, AKB and CDK1 were all in a tight range from 0.002 to 0.022 μM except for the compounds **11** and **14** which were a little weaker against CDK1. This strong biochemical activity gave rise to a marked phenotypic effect yielding G2/M arrest at concentrations between 0.01 and 0.03 μM. The HCT116 cell viability assay confirmed the potencies of these compounds in cells with IC₅₀s within the same range.

Furthermore, a matched analysis of three pairs of enantiomers in this series revealed that the (*S*) enantiomers were more potent than their corresponding (*R*) isomers, especially in the case of the primary alcohol **13a** which displayed enantiomeric-selectivity ratios of 25, 12 and 15 for AKA, AKB and CDK1, respectively (Table 4).

Table 2
SAR of 1-substituted-pyrazolopyrimidines

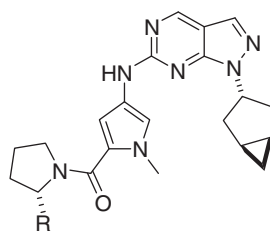


Compd	R ¹	AKA IC ₅₀ (μM)	AKB IC ₅₀ (μM)	CDK1 IC ₅₀ (μM)	G2/M ^a arrest (μM)	HCT116 IC ₅₀ (μM)	cLogP	MLM Stability (% Qh) ^b
7a		0.23	0.038	0.16	1	1	1.2	27
7b		0.15	0.019	0.05	0.65	0.29	2.1	89
7c		0.025	0.018	0.038	0.3	0.27	4.0	89
7d		0.021	0.012	0.016	0.3	0.23	2.7	76
7e		0.087	0.023	0.015	0.23	0.14	2.9	87
7f		0.04	0.005	0.019	0.3	0.12	2.7	89
7g		0.03	0.005	0.024	0.1	0.1	3.4	92
7h		0.017	0.004	0.024	0.1	0.079	1.6	69
7i		0.013	0.022	0.013	0.1	0.066	2.7	85

^a The G2/M arrest corresponds to the minimum concentration for G2/M versus G1 peak ratio over 2.

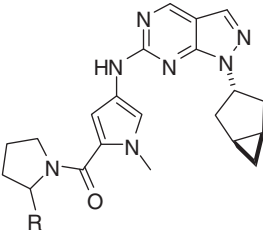
^b % Qh = in vitro clearance/hepatic blood flow of the species.

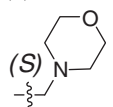
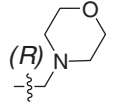
Table 3
SAR of 2-substituted-pyrrolidine amides **8** to **16a**



Compd	R	AKA IC ₅₀ (μM)	AKB IC ₅₀ (μM)	CDK1 IC ₅₀ (μM)	G2/M 100% (μM)	HCT116 IC ₅₀ (μM)
8	CONMe ₂	0.019	0.004	1.7	0.1	0.16
9	CH ₂ NHMe	0.08	0.05	1.2	0.3	0.15
10	Me	0.002	0.004	0.04	0.03	0.13
11	H	0.017	0.04	0.041	0.1	0.095
12	CONH ₂	0.006	0.004	0.01	0.03	0.047
13a	CH ₂ OH	0.004	0.003	0.010	0.01	0.018
14		0.01	0.005	0.047	0.03	0.011
15a	CH ₂ OMe	0.004	0.005	0.022	0.03	0.01
16a		0.003	0.004	0.021	0.017	0.008

Table 4
SAR of enantiomeric pairs of 2-substituted-pyrrolidine amides



Compd	R	AKA IC ₅₀ (μM)	AKB IC ₅₀ (μM)	CDK1 IC ₅₀ (μM)	G2/M 100% (μM)	HCT116 IC ₅₀ (μM)
13a	(S)CH ₂ OH	0.004	0.003	0.010	0.01	0.018
13b	(R)CH ₂ OH	0.1	0.036	0.15	0.1	0.17
15a	(S)CH ₂ OMe	0.004	0.005	0.022	0.03	0.01
15b	(R)CH ₂ OMe	0.016	0.006	0.15	0.065	0.06
16a		0.003	0.004	0.021	0.017	0.008
16b		0.0015	0.004	0.39	0.03	0.024

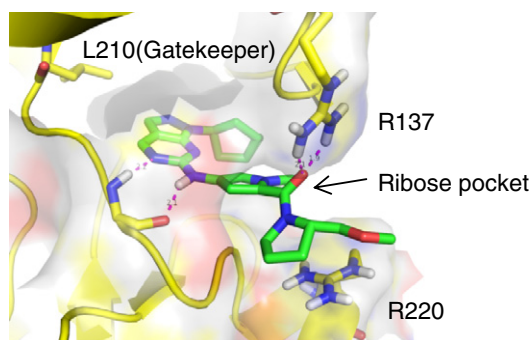


Figure 1. Docking of compound **15a** against AKA.

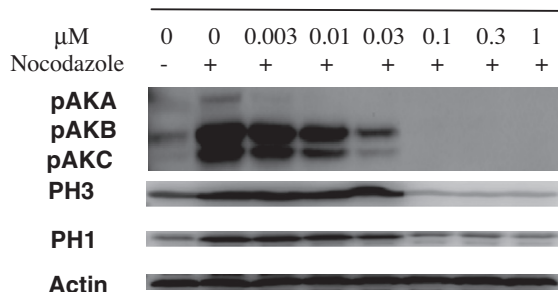


Figure 2. Effect of **15a** on the phosphorylation level of AKA, AKB and AKC in K562 cells.

The docking study for this series is exemplified in **Figure 1** showing the key interactions between **15a** and the ATP binding site of AKA. Two hydrogen bonds are predicted between the pyrazolo-pyrimidine core and the hinge region. More interestingly, the 2-methoxymethyl-pyrrolidine amide moiety binds in an optimal manner with the side-chains of Arg137 and Arg220 of AKA.¹¹ The *R*-methoxymethyl (**15b**) is expected to weaken this interaction. This moiety is also predicted to interact with Lys9 and Lys89 in CDK1.

Table 5
Selected pharmacokinetic parameters of **15a** in mouse and rat.

Dose (mg/kg)	T _{1/2} (h)	AUC (h ng/mL)	CL (mL/min/kg)	V _z (L/kg)
25 ^a	1	6416	65	3
4 ^b	5	1228	55	5

^a Mouse PK, intraperitoneal administration.

^b Rat PK, intravenous administration.

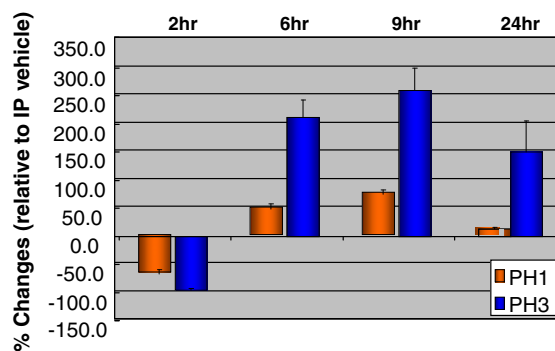


Figure 3. Pharmacodynamic experiment data for **15a** in mouse at low serum concentrations.

The kinase selectivity screening of **15a** against a panel of 262 kinases resulted in the inhibition of 100 kinases with IC₅₀ ≥ 1 μM, suggesting that the compound is very selective. To further determine whether the biochemical assay, which was performed without regulatory factors, was reflective of the *in vivo* pharmacodynamics, the levels of phosphorylation of AKA and AKB in cells were determined upon treatment of K562 leukemia cells with different concentrations of **15a**. Quantitation of the levels of phosphorylated Aurora kinases by Western blot shows that **15a** inhibits AKA phosphorylation at much lower concentrations than the concentrations required to fully inhibit AKB phosphorylation (**Fig. 2**). Possibly the discrepancies between the IC₅₀s observed in the biochemical assay and PD assay can be explained not including the co-factors TPX2 and INCENP in the AKA and AKB biochemical assays.

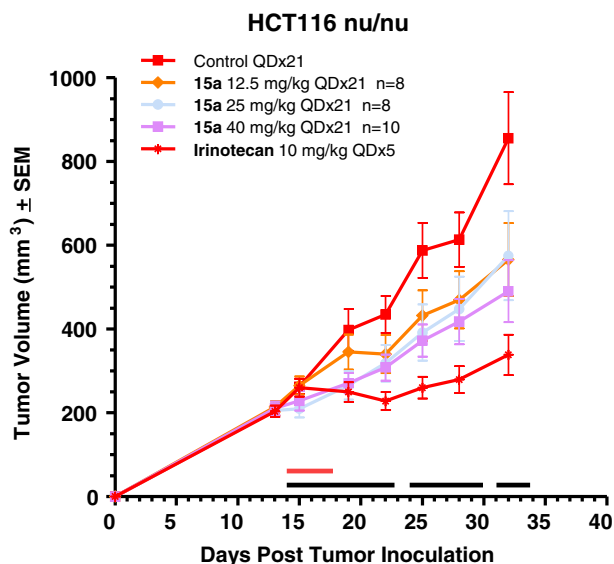


Figure 4. Efficacy study of **15a** in HCT116 nu/nu mouse models.

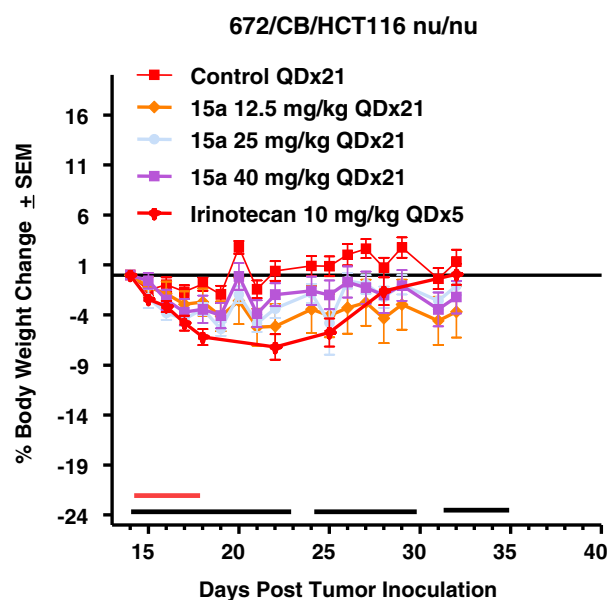


Figure 5. Body weight loss after administration of **15a** in HCT116 nu/nu mouse models.

Pharmacokinetic studies of **15a** in mice and rat showed that this compound exhibited medium to high clearance along with low distribution volumes (Table 5). Subsequently, a pharmacodynamic experiment confirmed the CDK1 inhibition phenotype at high serum concentrations (after 2 h) with 60% and 90% decreases in biomarkers phosphorylated histone H1 (pH1) and phosphorylated histone H3 (pH3), respectively. At lower serum concentrations (after 6 and 9 h), a dramatic increase in phosphorylated histone

H3 was observed, corresponding to an AKA inhibition phenotype as observed for AKA selective inhibitors such as MLN8054¹² (Fig. 3).

As **15a** displayed acceptable PK properties, was effective in modulating the AKA and CDK1 biomarkers and exhibited the highest neutropenic index of 32 (other data not shown), we conducted an efficacy study in the HCT116 nu/nu mouse models by administering it daily using IP route (Fig. 4). It resulted in modest tumor growth inhibition (30–40%) and moderate weight loss (2–9%) along with a range of side effects such as reluctance to move and hunched postures (Fig. 5). In addition, deaths of a few animals in this study indicated that **15a** was not tolerated at this dosing regimen.

In conclusion, the optimization of the SAR for this series against AKA, AKB and CDK1 has been achieved. The PK and PD studies on **15a** and other analogs (data not shown) revealed that this class of compounds reached serum levels which are sufficient to efficiently modulate the histone biomarkers pH1 and pH3 corresponding, respectively, to CDK1 and AKA inhibition phenotypes. However, the modest efficacy and the lack of tolerability in mouse models, probably due to both ubiquitous nature and medium clearance of this series, prevented us from evaluating this class of compounds any further.

Acknowledgments

Special thanks to Dr. Adeela Kamal, Dr. Srinivas R. Kasibhatla, Dr. Francis J. Burrows, and Dr. Marcus F. Boehm for their contributions to this program.

References and notes

- Lapenna, S.; Giordano, A. *Nat. Drug Disc.* **2009**, *8*, 547.
- Kitzen, J. J.; De Jonge, M. J.; Verweij, J. *Crit. Rev. Oncol. Hematol.* **2010**, *73*, 99.
- Andrews, P. *Oncogene* **2005**, *25*, 5005.
- Bayliss, R.; Sardon, T.; Vernos, I.; Conti, E. *Mol. Cell* **2003**, *12*, 851.
- Sessa, F.; Mapelli, M.; Ciferri, C.; Tarricone, C.; Areces, L. B.; Schneider, T. R.; Stukenberg, P. T.; Musacchio, A. *Mol. Cell* **2005**, *18*, 379.
- Emmanuel, S.; Rugg, C. A.; Gruninger, R. H.; Lin, R.; Fuentes-Pesquera, A.; Connolly, P. J.; Wetter, S. K.; Hollister, B.; Kruger, W. W.; Napier, C.; Jolliffe, L.; Middleton, S. *Cancer Res.* **2005**, *19*, 9038.
- Vanderwel, S. N.; Harvey, P. J.; McNamara, D. J.; Repine, J. T.; Keller, P. R.; Quin, J., III; Booth, R. J.; Elliott, W. L.; Dobrusin, E. M.; Fry, D. W.; Toogood, P. *L. J. Med. Chem.* **2005**, *48*, 2371.
- Zhang, L.; Fan, J.; Chong, J.-H.; Cesena, A.; Tam, B.; Gilson, C.; Boykin, C.; Wang, D.; Aivazian, D.; Marcotte, D.; Xiao, G.; le Brazidec, J.-Y.; Piao, J.; Lundgren, K.; Hong, K.; Vu, K.; Nguyen, K.; Gan, L.-S.; Silvan, L.; Ling, L.; Teng, M.; Reff, M.; Takeda, N.; Timple, N.; Wang, Q.; Morena, R.; Khan, S.; Zhao, S.; Li, T.; Lee, W.-C.; Taveras, A. G.; Chao, J. *Bioorg. Med. Chem. Lett.* **2011**, *21*, 5633.
- Leeson, P. D.; Springthorpe, B. *Nat. Rev. Drug Disc.* **2007**, *6*, 881.
- Cheatham, G. M. T.; Knegtel, R. M. A.; Coll, J. T.; Renwick, S. B.; Swenson, L.; Weber, P.; Lippke, J. A.; Austen, D. A. *J. Biol. Chem.* **2002**, *277*, 42419.
- The model of **15a** in AKA was generated using Glide 5.5 (Schrodinger, LLC) based on the published crystal structure of Aurora A (pdb: 3R21). Graphics generated in PyMol (Delano Scientific, South San Francisco, version 0.99).
- Manfredi, M. G.; Ecsedy, J. A.; Meetze, K. A.; Balani, S. K.; Burenkova, O.; Chen, W.; Galvin, K. M.; Hoar, K. M.; Huck, J. J.; LeRoy, P. J.; Ray, E. T.; Sells, T. B.; Stringer, B.; Stroud, S. G.; Vos, T. J.; Weatherhead, G. S.; Wysong, D. R.; Zhang, M.; Bolen, J. B.; Claiborne, C. F. *Proc. Natl. Acad. Sci. U.S.A.* **2007**, *104*, 4106.
- CFU-GM assay: Approximately 3.75×10^4 bone marrow mononuclear cells (Stem Cell Technologies) were plated in duplicate in Methocult media designed for CFU-GM assays of human cells containing rhSCF, rhG-CSF, rhGM-CSF, rhlL-3 containing vehicle or various concentrations of indicated drug. Colonies were allowed to form under humidified conditions at 37 °C, 5% CO₂ for 14 days. At which time, CFU-GM colonies were scored manually under light microscopy. EC₅₀s were determined by GraphPad analysis.